

# BFKL versus HERA

I. Bojak and M. Ernst

Institut für Physik, Universität Dortmund  
D-44221 Dortmund, Germany

## Abstract

The BFKL equation and the  $k_T$ -factorization theorem are used to obtain predictions for  $F_2$  in the small Björken- $x$  region over a wide range of  $Q^2$ . The dependence on the parameters, especially on those concerning the infrared region, is discussed. After a background fit to recent experimental data obtained at HERA and at Fermilab (E665 experiment), we find that the predicted, almost  $Q^2$  independent BFKL slope  $\lambda \gtrsim 0.5$  appears to be too steep at lower  $Q^2$  values. Thus there seems to be a chance that future HERA data can distinguish between pure BFKL and conventional field theoretic renormalization group approaches.

# 1 Introduction

The usual kinematic variables used for discussing deep-inelastic electron-proton scattering are derived from the four-momenta  $p$  of the incoming proton and  $q$  of the exchanged virtual photon:  $Q^2 \equiv -q^2$  and the Bjørken variable  $x \equiv Q^2/2p \cdot q$ . In the region where higher twist effects are likely to be negligible, i. e., for  $W^2 \equiv Q^2(1/x - 1) \gtrsim 10 \text{ GeV}^2$ , the (Dokshitzer-Gribov-Lipatov-)Altarelli-Parisi [(DGL)AP] set of equations [1, 2] describes the evolution of the structure function  $F_2$  with  $Q^2$  very well. In leading order (LO) all powers of  $\alpha_s \ln(Q^2/\mu^2)$  are summed by the AP evolution equations, which take into account just strongly ordered parton- $k_T$  ladders. Nowadays usually the next-to-leading order (NLO) set is used, where terms of the form  $\alpha_s^n \ln^{n-1}(Q^2/\mu^2)$  are also summed, taking *non*-ordered  $k_T$  contributions (covariantly) into account as well. Even in NLO, the AP equations do obviously not contain all leading logarithms in  $x$ . Thus one might naïvely expect the AP framework to break down at some small value of  $x$ , where a resummation of all powers of  $\alpha_s \ln(1/x)$  should be necessary, although no perturbative instability between LO and NLO has been observed thus far in the presently relevant kinematic regime [3, 4, 5].

Such a resummation in LO is provided by the Balitskij-Fadin-Kuraev-Lipatov (BFKL) equation [6]. The equation treats the gluons only, which are expected to be the dominant partons at small  $x$ . This might be deduced from the AP splitting functions [1], which become  $\sim 1/x$  for splitting to gluons and constant for splitting to quarks in the small  $x$  limit. It should be remarked though, that this argument may be too simple, as it neglects the influence of the particular shape of the parton distributions used [4, 5] and furthermore does not respect the fundamental energy-momentum conservation constraint. The BFKL resummation is formally correct for all  $Q^2$ , but a fixed coupling  $\bar{\alpha}_s$  was used in its derivation. Furthermore it is based on LO perturbative QCD, using (non-covariant)  $k_T$  cut-off regularizations, thus we are limited to sufficiently large  $Q^2$ . Since the resummation assumes that subleading terms in  $x$  are small, including those involving logarithms of  $Q^2$ , it will also not be valid at high  $Q^2$ . A conservative range for  $Q^2$  would be 4 to 50  $\text{GeV}^2$ , and the range 0.8 to 120  $\text{GeV}^2$  explored in this work should be regarded as the extreme

limit.

To estimate the effects of the subleading terms, a NLO resummation in  $x$  would be necessary. But even though there has been some progress in that direction [7], a final result has not yet been obtained. Ultimately it should even be possible to find a unified evolution equation covering the whole perturbative region [8, 9, 10]. But a calculation that can be confronted with experiment is still missing, thus we stay with the usual BFKL formalism for the time being.

Since a fixed coupling constant seems unreasonable in view of the running coupling of the AP framework we wish to connect to, the replacement  $\bar{\alpha}_s \rightarrow \alpha_s(Q^2)$  is done by hand. There is really no rigorous motivation for this step. Some trust in this procedure can be gained by considering the representation of the evolution equations as ladder diagrams. It is well known that the LO AP equations can be represented in a physical gauge by a sum of ladder graphs which are strongly ordered in the transverse momentum  $k^2$ :  $Q^2 \gg k^2 \gg k_{n-1}^2 \gg \dots \gg k_1^2 \gg k_0^2$ . In the small  $x$  limit of the AP equation we consider only the dominant gluon ladder (see Fig. 1) and keep only the terms with double leading logarithms (DLL)  $\alpha_s \ln(1/x) \ln(Q^2/\mu^2)$ . This corresponds to introducing an additional strong ordering in  $x$ :  $x \ll x_{n-1} \ll \dots \ll x_0$ . The BFKL evolution can also be described in terms of a (reggeized) gluon ladder, using the strong ordering in  $x$  only, to get the leading logarithms in  $x$ . If we let the coupling run, then BFKL will reduce to LO DLL upon imposing the ordering in transverse momentum.

The main feature of the BFKL evolution with fixed coupling constant  $\bar{\alpha}_s$  is the growth of the unintegrated gluon  $\sim x^{-\lambda}$  with  $\lambda = \frac{3\bar{\alpha}_s}{\pi} 4 \ln 2 \simeq 0.5$ . Due to the dominance of the gluons at small  $x$  we expect a corresponding rise at small  $x$  in the structure functions too, once the off-shell gluons have been appropriately coupled to the quark sector. This expectation has been confirmed [11, 12] for a small range of medium  $Q^2$  even in the case of running coupling BFKL, with  $F_2 \sim x^{-\lambda}$  and  $\lambda \gtrsim 0.5$  for  $x < 10^{-3}$ .

Experimentally the situation has improved drastically since the advent of the HERA *ep*

collider. Before HERA only the Fermilab experiment E665 [13] was able to reach the small  $x$  region, but at rather low  $Q^2$ . Now HERA takes data [14, 15] with  $x/Q^2 \gtrsim 3 \cdot 10^{-5}$  over a wide range of  $Q^2$ . The observed strong rise of  $F_2$  at small  $x$  has boosted the interest in the BFKL formalism. On the other hand the dynamically generated AP partons [5] create a steep gluon distribution, via a long evolution length in  $Q^2$ , and successful parameter-free predictions [3, 5, 16] have been given long before HERA started to operate. Alternatively, the present data can be fitted using the NLO AP evolution equations: Then a term  $\sim x^{-\lambda}$  has to be *assumed* for the gluon distribution, e. g. in MRSG [17]. Possibly this term mimicks the BFKL behaviour. But this is not clear, since both methods describe the data equally well.

We conclude that a detailed comparison of the standard BFKL formalism with the new data is necessary. Only this can tell us if BFKL can rival conventional field theoretic renormalization group (AP) evolution equations in describing the measured structure function  $F_2$ . Our calculations are based on the methods employed by Askew, Kwieciński, Martin and Sutton (AKMS) [11, 12, 18], which will be described briefly in the following.

## 1.1 BFKL equation and $k_T$ -factorization

The unintegrated gluon distribution  $f(x, k^2)$ , which is related to the familiar integrated gluon distribution used in the AP equations by

$$x g(x, Q^2) = \int_0^{Q^2} \frac{dk^2}{k^2} f(x, k^2), \quad (1a)$$

$$f(x, k^2) = \left. \frac{\partial x g(x, Q^2)}{\partial \ln(Q^2)} \right|_{Q^2=k^2}, \quad (1b)$$

depends on the transverse momentum  $k$ . Using it, one can write the BFKL equation as [19]

$$f(x, k^2) = f_0(x, k^2) + \int_x^1 \frac{dy}{y} \int dk'^2 K(k^2, k'^2) f(y, k'),$$

$$K(k, k') = \frac{3\alpha_s(k^2)}{\pi} k^2 \left\{ \frac{1}{k'^2 |k^2 - k'^2|} - \beta(k^2) \delta(k^2 - k'^2) \right\},$$

$$\beta(k^2) = \int \frac{dk'^2}{k'^2} \left\{ \frac{1}{|k^2 - k'^2|} - \frac{1}{(4k'^4 + k^4)^{\frac{1}{2}}} \right\}.$$

One could use a suitable input  $f_0$ , the so called “driving term”, and solve the equation iteratively [10], but this procedure allows no simple connection to the known AP region.

Instead we can obtain an evolution equation in  $x$  from the integral equation by differentiating with respect to  $\ln(1/x)$

$$-x \frac{\partial f(x, k^2)}{\partial x} = \frac{3\alpha_s(k^2)}{\pi} k^2 \int \frac{dk'^2}{k'^2} \left[ \frac{f(x, k'^2) - f(x, k^2)}{|k'^2 - k^2|} + \frac{f(x, k^2)}{(4k'^4 + k^4)^{\frac{1}{2}}} \right], \quad (2)$$

assuming that the derivative of the driving term  $f_0$  can be neglected. Since the driving term describes the gluon content without any BFKL evolution, it is reasonable to assume that it is connected to the non-perturbative “soft” pomeron [20]. Because of the soft pomeron’s weak  $x$  dependence  $\sim x^{-0.08}$ , we expect  $\partial f_0 / \partial \ln(1/x)$  to be small.

Eq. (2) can then be used to evolve the unintegrated gluon to smaller  $x$ , using a suitably modified AP input as boundary condition at  $x_0 = 10^{-2}$  by applying Eq. (1a). An obvious problem in Eq. (2) is posed by the integration over  $k'^2$ , which starts at zero. Even for the AP gluon distributions we use in this work the limit of validity is about 1 GeV<sup>2</sup>. We employ a simple ansatz to continue the gluon into the infrared (IR) region, which will be described later in this paper. A similar comment applies to the upper limit of the  $k'^2$  integration. The upper limit introduced by energy conservation is close to infinity [11, 12], so that for practical calculations an artificial ultraviolet cutoff has to be introduced. The dependence on the IR and UV treatment will be thoroughly discussed later on.

To obtain predictions for  $F_2$ , we have to convolute the (off-shell) BFKL gluon, i. e. the gluon ladder in Fig. 1, with the photon-gluon fusion quark box  $F^{(0)}$  using the  $k_T$ -factorization theorem [9, 21]

$$F_i(x, Q^2) = \int \frac{dk'^2}{k'^4} \int_x^1 \frac{dy}{y} f\left(\frac{x}{y}, k'^2\right) F_i^{(0)}(y, k'^2, Q^2), \quad (3)$$

with  $i = T, L$  denoting the transverse and longitudinal parts, respectively. The expressions for  $F^{(0)}$  can be found in [18] and references therein. The BFKL prediction for  $F_2$  is then

simply the sum of the calculated  $F_T$  and  $F_L$ . Obviously here the same problems with the  $k'^2$  integration occur, which are circumvented by the methods mentioned above.

It is important to notice that the BFKL gluons are *off-shell* ( $k^2 \neq 0$ ). The term  $F^{(0)}/k^2$  in the above equation then corresponds to the structure function of a virtual gluon. In contrast the AP formalism is based on *on-shell* gluons, which is a good approximation due to the strong ordering in transverse momentum encountered in AP evolutions in LO. This strong ordering allows us to perform the  $k'^2$  integration in Eq. (3). Thus, ignoring complications due to the collinear singularities for simplicity, one arrives at the usual mass factorization equation

$$F_i(x, Q^2) = \int_x^1 \frac{dy}{y} g\left(\frac{x}{y}, Q^2\right) \hat{F}_i(y, Q^2).$$

Here  $\hat{F}_i$  plays the rôle of the on-shell gluon structure function, whose  $x$  dependence stems from the AP splitting function  $P_{gg}$ , and  $g$  is the integrated gluon. In NLO AP evolutions the strong ordering in  $k^2$  does not hold anymore due to the emission of a second gluon, but the interacting gluon is still considered to be on-shell in comparison with the hard scattering scale  $Q^2$ .

This shows that it is inconsistent to simply feed the evolved BFKL gluon via Eq. (1a) back into the AP equations below the limit set by  $x_0$ . Calculations attempting to use BFKL gluons below and AP gluons above  $x_0$  within the AP formalism [22] ignore the essential *off-shellness* of the BFKL gluons. This casts first doubts on a recent BFKL analysis of the HERA H1 data using this method [23]. No such problem persists when we use just this gluon mixture to drive the general  $k_T$ -factorization Eq. (3), which reduces to the mass factorization in the AP region.

Even though the dominant contribution at small  $x$  should come from the BFKL gluons, a certain amount of “background” in  $F_2$  due to quarks and non-perturbative effects should be taken into account. We expect the background to be comparatively small and also to vary much less with  $x$ . We shall use an ansatz motivated by the soft pomeron  $C_{IP} x^{-0.08}$ , where the constant  $C_{IP}$  is fitted to the data. After this general outline of our method, we

will now proceed to a detailed discussion of the underlying formalism.

## 2 Suitable input for the BFKL evolution

We focus our analysis on the gluon distribution used in [12], i.e. a gluon based on the MRS  $D_0$ -set of parton distributions [24], but evolved with the leading order Altarelli-Parisi equations [25]. Since the BFKL evolution deals with an *unintegrated* gluon distribution, we calculate its derivative using the well-known singlet Altarelli-Parisi equation given by

$$f^{\text{AP}}(x, Q^2) = \frac{\alpha_s(Q^2)}{2\pi} \int_x^1 \frac{dy}{y} \left( P_{gg}^{(0)}\left(\frac{x}{y}\right) g(y, Q^2) + P_{gq}^{(0)}\left(\frac{x}{y}\right) \Sigma(y, Q^2) \right),$$

where  $\Sigma$  denotes the quark singlet part, and  $P_{gg}^{(0)}$ ,  $P_{gq}^{(0)}$  the usual LO splitting functions. In the same way we produce a leading order MRS  $D_-$ -type gluon, based on an input given in [26].

We also use a dynamically generated gluon distribution, for definiteness the GRV '92 LO parametrization [3], that has the advantage of (a) being based on an explicit LO calculation and (b) being positive definite down to a low value of  $Q^2$ .

Furthermore, we take a look at the MRSA-Low  $Q^2$  gluon [27], which extends the valid  $Q^2$  range down to  $0.625 \text{ GeV}^2$  using an ad hoc form-factor-like ansatz similar to the one we employ for  $f$ . However, as MRSA is a NLO analysis, there is no consistent way to implement it in our BFKL evolution, which is neither an  $\overline{\text{MS}}$ - nor DIS-renormalization scheme calculation.

### 2.1 Treatment of the infrared region

As mentioned in the Introduction, we need a suitable description of the infrared region; for our calculations we use the ansatz explained in detail in [11, 12]. This ansatz introduces three parameters:

- An IR-“cutoff”  $k_c^2$ , i.e. a parameter which separates the infrared region, where an assumption on the  $k^2$ -behaviour of  $f$  has to be made, from the region where the Lipatov equation is solved numerically.
- A parameter  $k_a^2$  that controls the infrared behaviour of  $f$ . For  $k^2 < k_c^2$  we set:

$$f(x, k^2) = C' \frac{k^2}{k^2 + k_a^2} f(x, k_c^2). \quad (4)$$

The proportionality constant is given by

$$C' = \frac{k_c^2 + k_a^2}{k_c^2},$$

to guarantee continuity at  $k^2 = k_c^2$ . This ansatz ensures that for  $k^2 \rightarrow 0$ ,  $f(x, k^2) \sim k^2$ , as required by gauge invariance.

- A scale  $k_b^2$  where we “freeze” the running coupling constant, i.e.

$$\alpha_s(k^2) \longrightarrow \alpha_s(k^2 + k_b^2).$$

This procedure applies also to our boundary condition  $f(x_0, k^2)$ , although there is a slight modification to the pure AP gluon in order to soften its low  $k^2$  behaviour:

$$f^{\text{AP}}(x_0, k^2) \longrightarrow f^{\text{AP}}(x_0, k^2 + k_s^2). \quad (5)$$

The only purpose of the additional parameter  $k_s^2$  is to ensure that we do not approach too closely a region where the gluon is unreliable; e.g. the  $D_0$ -type gluon already approaches zero at  $Q^2 = 1 \text{ GeV}^2$ , and the  $D_-$ -type gluon is not defined at all for such a low scale.

Thus,

$$f(x_0, k^2) = \begin{cases} \left( \frac{k^2}{k^2 + k_a^2} \right) f^{\text{AP}}(x_0, k_c^2 + k_s^2) & \text{for } k^2 < k_c^2 \\ \left( \frac{k^2}{k^2 + k_a^2} \right) f^{\text{AP}}(x_0, k^2 + k_s^2) & \text{for } k^2 \geq k_c^2. \end{cases} \quad (6)$$

This provides an infrared behaviour according to (4), and for  $k^2$  large enough  $f(x_0, k^2)$  approaches  $f^{\text{AP}}(x_0, k^2)$ .



In ref. [11], the parameter  $k_s^2$  is set equal to  $k_a^2$ , whereas in [12]  $k_s^2$  equals  $k_b^2$ . We prefer setting  $k_s^2 = k_a^2$  for reasons given below.

## 2.2 Fixing $k_a^2$

It seems to be clear that the parameters introduced above should be small; so the simplest choice for these would be [12]:

$$k_a^2 = k_b^2 = k_c^2 = k_s^2 = 1 \text{ GeV}^2. \quad (7)$$

However, there is a self-consistency constraint on the choice of  $k_a^2$ , depending on  $k_c^2$  and  $x_0$ . The boundary condition (6) should inversely be related to the (integrated) Altarelli-Parisi gluon  $g$  in Eq. (1a), that is

$$x_0 g(x_0, Q^2) - \int_0^{Q^2} \frac{dk^2}{k^2} f(x_0, k^2) = 0. \quad (8)$$

In a stricter approach, we apply the shift introduced in (5) also to the integrated gluon  $g$  in this equation. Then it is not very difficult to show that

$$\int_{k_c^2+k_a^2}^{Q^2+k_a^2} dl^2 \left( 1 + \frac{k_s^2 - k_a^2}{l^2} \right) \frac{\partial x_0 g(x_0, Q^2)}{\partial Q^2} \Big|_{Q^2=l^2+k_s^2-k_a^2} = x_0 g(x_0, Q^2+k_s^2) - x_0 g(x_0, k_c^2+k_s^2). \quad (9)$$

It is obvious that this equation is fulfilled by setting  $k_s^2 = k_a^2$ , hence motivating our previous assumption. Using this and the asymptotic behaviour of  $g$ ,

$$x g(x, Q^2 + k_s^2) \stackrel{Q^2 \gg k_s^2}{\simeq} x g(x, Q^2), \quad (10)$$

we may return to (8) for simplicity, which gives us upon inserting our boundary condition (6)

$$\begin{aligned} x_0 g(x_0, Q^2) &= \int_0^{k_c^2} \frac{dk^2}{k^2 + k_a^2} f^{\text{AP}}(x_0, k_c^2 + k_a^2) + \int_{k_c^2}^{Q^2} \frac{dk^2}{k^2 + k_a^2} f^{\text{AP}}(x_0, k^2 + k_a^2) \\ &\simeq f^{\text{AP}}(x_0, k_c^2 + k_a^2) \ln \frac{k_c^2 + k_a^2}{k_a^2} + x_0 g(x_0, Q^2) - x_0 g(x_0, k_c^2 + k_a^2). \end{aligned}$$

Set	$\Lambda_{\text{QCD}}^{(4)}$ [MeV]	$x_0$	$k_c^2$ [GeV <sup>2</sup> ]	$k_a^2$ [GeV <sup>2</sup> ]
$D_0$ -type	173.2	0.01	1.0	0.95
$D_-$ -type	230.4	0.01	1.0	1.51
GRV '92-LO	200.0	0.01	1.0	0.19
MRSA-Low $Q^2$	230.0 ( $\overline{\text{MS}}$ )	0.01	1.0	0.44

Table 1: Parameters for various sets of parton distributions

Thus we obtain an implicit equation for  $k_a^2$ :

$$\ln \frac{k_c^2 + k_a^2}{k_a^2} \simeq \frac{x_0 g(x_0, k_c^2 + k_a^2)}{f^{\text{AP}}(x_0, k_c^2 + k_a^2)}. \quad (11)$$

One can see that the value of  $k_a^2$  mainly depends on the ratio  $g/f$  in the region of low  $Q^2$ , and as the variation of  $f$  for different parton distributions is relatively small in that region compared to the variation of  $g$ , we conclude that it is basically the absolute value of  $g$  that determines the size of  $k_a^2$ . Hence, as a rule of thumb, the higher the value of  $x_0 g(x_0, Q^2)$  for small  $Q^2$ , the smaller the resulting  $k_a^2$ . It should be emphasized that, although the shift in Eq. (5) is taken into account in Eq. (9) for both  $f$  and  $g$ , but in Eq. (11) only for  $f$ , the solution of Eq. (11) provides a good estimate on  $k_a^2$ , very close to the value we get by minimizing the l.h.s. of Eq. (8) for  $Q^2 > 100$  GeV<sup>2</sup>. The result for all the parton distributions under consideration is given in Table 1, together with the value of  $\Lambda_{\text{QCD}}$  for four flavors used with each distribution. Figure 2 shows the unmodified gluons and the modified boundary conditions according to Table 1.

Regarding the  $D_0$ -type gluon, we see that the optimized value of  $k_a^2 = 0.95$  GeV<sup>2</sup> is indeed very close to the naïve estimate of 1 GeV<sup>2</sup>, as was already noticed in [12]. It was also mentioned there that a reasonable choice of  $k_a^2$  should lie in the range of 0.5 – 2 GeV<sup>2</sup>, and we see that the  $D_-$ -type value lies well within this range, while the MRSA set is already close to its lower edge. The most extreme boundary condition in this respect is derived from the GRV parametrization, with a value of only 0.19 GeV<sup>2</sup>.

As the more recent parton distributions favor a larger gluon  $g$ , the assumption of  $k_a^2 = 1$  GeV<sup>2</sup> (a good choice for the relatively small  $D_0$ -type gluon) does not appear to be

the best choice for these gluons.

Let us now emphasize the importance of the constraint (8) on  $k_a^2$ : Starting with the simple assumption (7) that all the parameters introduced should be equal to  $1 \text{ GeV}^2$ , one gets a slope

$$\lambda = \frac{1}{f} \frac{\partial f}{\partial \ln(1/x)} \Big|_{x=10^{-4}} = 0.5 - 0.6$$

for the unintegrated, BFKL evolved gluon distribution, as expected, no matter if  $D_0$ -type,  $D_-$ -type, or GRV is chosen as input for the BFKL evolution. If we deviate each of the infrared parameters from (7), we see that it is  $k_a^2$  which has the biggest impact on  $\lambda$ . With  $k_a^2$  decreasing, the slope rises, resulting in a slope  $\lambda \simeq 0.9$  for GRV partons ( $k_a^2 = 0.19 \text{ GeV}^2$ ) as the extreme limit.

Keeping these considerations in mind, we will now concentrate our analysis on the structure functions. We will demonstrate that the slopes of  $f$  and  $F_2$  are related in such a way that for large  $\lambda$  our calculated  $F_2$  is too steep to match it to the recent HERA data.

### 3 Varying the parameters

We construct the boundary condition at  $x_0 = 10^{-2}$ . The consistency constraint (8) determines  $k_a^2$  and as a standard value for the other two IR parameters we choose  $k_b^2 = k_c^2 = 1 \text{ GeV}^2$ . The UV cutoff is set to  $10^4 \text{ GeV}^2$  and we stay with the  $\Lambda_{\text{QCD}}$  of the AP partons. We have written an evolution program to solve (2) iteratively. Below  $k_c^2$  the necessary integration can easily be done analytically, above we use the Gauß-Legendre quadrature. This transforms the integro-differential equation (2) into a set of coupled differential equations, allowing us to use the standard Runge-Kutta method to calculate the evolution. The evolved gluon below  $x_0$  is combined with the unintegrated AP gluon above  $x_0$  to obtain predictions for  $F_T$  and  $F_L$  by performing the integration in Eq. (3) with Monte-Carlo methods. For convenience a fit of  $F_2 = F_T + F_L$  is given in the Appendix. Finally we fit the background to the data, as discussed at the end of Section 1.1, and

obtain our BFKL prediction.

It is vital to check the dependence of the results on the parameters used for the IR and UV treatment. In Fig. 3 we varied all relevant parameters, using the  $D_0$ -type gluon. All curves have been calculated at  $Q^2 = 15 \text{ GeV}^2$  and are already fitted to the shown HERA data with the soft pomeron background  $C_{IP} x^{-0.08}$ .

The strong dependence on  $k_a^2$ , which we expect from the corresponding variation in the gluon slope, is obvious. The curves for low  $k_a^2$  are much too steep. At  $k_a^2 = 0.2 \text{ GeV}^2$  for example, the pure BFKL prediction is too high, even without any background. A background fit would then give a *negative* contribution, i. e.  $C_{IP} < 0$ , which is unphysical. In all such cases we set the background to zero. It is crucial, that  $k_a^2$  can be precisely determined from the consistency constraint. Without the constraint, we could vary the slope of  $F_2$  from 0.5 to 0.8 by choosing  $k_a^2$  within the shown range of 0.2 to 2.0  $\text{GeV}^2$ , rendering any serious prediction impossible. In the already mentioned comparison of a BFKL calculation with HERA data [23],  $k_a^2$  is treated as a *free* parameter. If the fitted  $k_a^2$  should not be close to the consistent value by chance, it is doubtful that any strong conclusions can be drawn from a successful description of the data.

The influence of the IR cutoff  $k_c^2$  is comparably small. It should be kept in mind that  $k_a^2$  has to be fitted separately for each  $k_c^2$ . Actually the induced variations in  $k_a^2$  dampen the dependence of the predictions on  $k_c^2$  slightly. It is no surprise, that variations of the UV cutoff do not introduce much uncertainty into the predictions, as the running coupling already serves as an effective UV cutoff [11, 12]. The remaining free IR parameter,  $k_b^2$ , has a sizeable effect on the curves. The slope of  $F_2$  varies from 0.53 to 0.58 in the shown  $Q^2$  range. The standard value of 1  $\text{GeV}^2$  gives a slope of about 0.55, and the variations of  $k_b^2$  represent an effective error-band of our calculations.

A considerable dependence on  $\Lambda_{\text{QCD}}$  is expected and can be seen in Fig. 3. Fortunately this parameter is fixed, since we are using AP gluons with a given  $\Lambda_{\text{QCD}}$  as boundary condition. It is interesting to note, that higher values of  $\Lambda_{\text{QCD}}$  than the rather low 173.2

MeV used in the  $D_0$ -type partons give *unfavourably* steep slopes! Finally we take a look at variations of  $x_0$ , noting that we have to determine  $k_a^2$  separately again. We expect the steep curve for  $x_0 = 5 \cdot 10^{-2}$  due to the long evolution length in  $x$ . But it is daring to use the BFKL equations at such high values of  $x$  and the data do not support such a choice. We can also see that the comparably flat curve created by a short evolution in  $x$  starting from  $x_0 = 10^{-3}$  does fit the data well. But this success can obviously not be claimed by the BFKL evolution, since the data do not extend far below that  $x_0$ . In order to test if the BFKL equations can describe the *current* data, we have to choose a larger  $x_0 \sim 10^{-2}$ . The typical steep BFKL slope simply needs enough evolution length to develop. Small variations to lower  $x_0$  from the usually used  $10^{-2}$  do not affect the calculations strongly. The standard values [11, 12] used for  $k_b^2$  and  $x_0$  give slopes slightly below and above the average expected from the variations, respectively. Thus this choice of parameters will give a sensible prediction while still allowing comparisons with earlier calculations [11, 12].

The results presented in this sections show that the dependence of the calculations on the parameters is under control. This statement would be impossible, if  $k_a^2$  did not obey the consistency constraint (8).

### 3.1 Using other input distributions

Besides our detailed analysis of the  $D_0$ -type gluon, we also studied the effect of feeding different parton distributions into our evolution, namely GRV'92 LO [3] and MRSA-Low  $Q^2$  [27]. The results for  $F_2$  can be seen in Fig. 4.

Obviously by using GRV and MRSA gluons as inputs for the BFKL evolution, a structure function is generated which is far too steep for the data. Even though we have got, in principle, some freedom in fitting an appropriate background, this is useless here, since already the pure BFKL part of  $F_2$  is too high for the HERA data, so that we must set the background to zero.

The steepness of  $F_2$  is closely related to the fact that the proper  $k_a^2$  is much smaller than  $1 \text{ GeV}^2$ , resulting in a larger slope  $\lambda$  of the BFKL gluon  $f$ . As we explained above, this is mainly an effect of the size of the integrated gluon input  $g$ . This suggests the conclusion that the whole BFKL procedure has only a chance to work with the older (smaller) gluons. Modern parton distributions imply small values of the crucial infrared parameter  $k_a^2$ , and since this has a strong effect on the calculated structure functions, it is likely that one does not succeed in matching these to present experimental data.

## 4 Comparison with data

In Fig. 5 we compare our calculations with very low  $Q^2$  data from the Fermilab E665 experiment [13]. Preliminary data of the HERA  $ep$  collider [15] at low  $Q^2$  are also shown in this figure. The published 1993 HERA data [14] for low to medium  $Q^2$  are presented in Fig. 6 together with our BFKL predictions. All graphs show the BFKL calculations based on the  $D_0$ -type and the  $D_-$ -type partons, as well as the latest dynamical NLO renormalization group predictions (GRV), as presented in [5]. Also shown is the soft pomeron background, which is included in the  $D_0$ -type curve. A general feature of all figures is that the difference between the  $D_0$ -type and the  $D_-$ -type BFKL predictions is very small after fitting the background. For this reason we do not discuss them separately. We have checked, that the  $R = F_L/F_T$  values used to extract  $F_2$  from the experimental data are close enough to those predicted by BFKL. Thus it is not necessary to reanalyze the data in terms of  $R_{\text{BFKL}}$ .

We first turn our attention to the E665 data [13]. The data do not extend very far into the small  $x$  region, making a check of the BFKL behaviour difficult. On the other hand the difference between the GRV (AP) and BFKL predictions is potentially large at small  $x$ . We also notice that the added background is comparable in size to the BFKL part at higher  $x$ . This flattens the steep BFKL behaviour, giving a good description of the data. But it is just the large contribution of the background which makes the very

procedure used doubtful.

A further hint, that the successful description of the E665 data should not be taken too seriously, is provided by comparing the curves for the E665 data at  $2.8 \text{ GeV}^2$  and those for preliminary ZEUS data at  $3.0 \text{ GeV}^2$ . While the E665 background is strong ( $C_{IP} = 0.189$ ) for  $D_0$ -type, the optimal ZEUS background would be negative ( $C_{IP} = -0.172$ ) and therefore is set to zero. Thus the natural requirement, that the BFKL predictions for similar  $Q^2$  values should be approximately equal, is only fulfilled at very small  $x$ . For  $x \gtrsim 10^{-4}$  the influence of the background quickly becomes stronger and the curves deviate. We conclude that BFKL can *not* describe both data sets consistently. It is also obvious from the figures that just this is possible using the usual NLO renormalization group equations, see the curves labeled GRV '94 in Fig. 5.

Turning to the preliminary HERA data in Fig. 5, we find that the BFKL slope of  $F_2$  is evidently too steep. The same tendency can also be found in the 1993 HERA data up to approximately  $15 \text{ GeV}^2$  as shown in Fig. 6. Everywhere in this region the background is very small or would even be negative, if it were allowed. Due to the larger spread in  $x$ , the preliminary data show the discrepancy rather clearly. The problem is rooted in the almost  $Q^2$  independent slope of BFKL, which is always  $\gtrsim 0.5$  and grows weakly with  $Q^2$ . The dynamical GRV (AP) calculations give on the contrary flat slopes at low  $Q^2$ , which rise significantly with larger  $Q^2$ . This is obviously in much better agreement with the data. For example, using the preliminary ZEUS data at  $4.5 \text{ GeV}^2$ , we get a total  $\chi^2$  of 15.3 ( $D_0$ -type), 15.0 ( $D_-$ -type) and of 2.81 (GRV '94 NLO) for the four data points.

At  $Q^2$  higher than  $15 \text{ GeV}^2$ , we see that the slope of the data becomes compatible with the one predicted by BFKL. The rising slope of the dynamical GRV prediction fits the data at least as well. It is interesting to note that even at higher  $Q^2$  a slight extension in the  $x$  range could provide an indication which evolution should be used. If future data should conform to the already visible tendency that a Lipatov-like slope is only obtainable at high  $Q^2$ , say  $\gtrsim 50 \text{ GeV}^2$ , then the simple LO BFKL formalism would

become implausible, since its validity at such high  $Q^2$  is questionable.

## 5 Conclusions

We have shown that the AKMS method for calculating BFKL predictions of  $F_2$  remains stable under variations of the introduced parameters, if the consistency constraint Eq. (8) on  $k_a^2$  is applied. As boundary conditions one has to choose older, i. e. smaller, gluon densities, since the large recent AP gluons lead to small  $k_a^2$ , which in turn produces overly steep slopes of  $F_2$ . The BFKL boost at small  $x$  is simply too large for gluons constructed to produce the measured large  $F_2$  slope via the conventional renormalization group (AP) evolution equations.

Thus we use the old  $D_0$ -type and  $D_-$ -type gluons with consistently fixed  $k_a^2$  as input for the BFKL evolution. A further complication is introduced by the necessity to add a background contribution to the BFKL prediction for  $F_2$ . Then it seems reasonable to require that the main growth of  $F_2$  is not driven by the chosen background, and that this background is comparably small. The last condition is not fulfilled in the region of the E665 experiment, casting serious doubts on the good agreement with the data.

In the HERA region we find in contrast small background contributions, allowing for reliable comparisons with experiment. Especially the preliminary HERA data in Fig. 5 show that the almost  $Q^2$  independent BFKL slope is too steep for  $Q^2 \lesssim 15 \text{ GeV}^2$ . But even up to the expected limit of applicability in  $Q^2$  of the BFKL evolution we find that the predicted slope is somewhat too steep. With improved statistics and maybe a slightly extended coverage in  $x$ , HERA should be able to assess the LO BFKL predictions for  $F_2$ . If the tendency visible in the current data is an indication for future developments, we expect LO BFKL to fail the test. It remains to be seen whether extensions of LO BFKL — inclusion of the quark sector, NLO BFKL or theoretically consistent (energy-momentum conservation, etc. ) unified evolution equations — can improve the agreement



with the data. Our results also indicate that conventional (dynamical) renormalization group evolutions are still the best method for calculating and analyzing  $F_2$ .

## 6 Acknowledgments

We are grateful to E. Reya and M. Glück for helpful guidance and fruitful discussions, and to E. Reya, M. Stratmann and S. Kretzer for carefully reading the manuscript. We thank P. J. Sutton for making the  $D_0$ -type partons available to us. I. B. wishes to thank D. Wegener for unbureaucratically granting additional computing time on his workstations. This work has been supported in part by the 'Bundesministerium für Bildung, Wissenschaft, Forschung und Technologie', Bonn.

## Appendix: Parametrization

It should be convenient to have a simple parametrization of our theoretical results for  $F_2$ . The following is a parametrization of the BFKL part only, to which an appropriate background still has to be added.

We use an ansatz of the form:

$$F_2^{BFKL} = \alpha x^{-\lambda} + \beta x + \gamma, \quad (\text{A.1})$$

which describes all curves shown in Figs. 3 – 6 well. It is even possible to parametrize *all* pure BFKL results for the  $D_0$ -type and  $D_-$ -type gluons shown in Figs. 5 and 6 by choosing the following  $Q^2$  dependence of the coefficients [ $t = \ln(Q^2/\Lambda_{\text{QCD}}^2)$ ]

$$\begin{aligned} \alpha(Q^2) &= A + Bt + Ct^2 + Dt^3, \\ \beta(Q^2) &= Et^2 + Ft^3, \\ \gamma(Q^2) &= G + H(Q^2/\text{GeV}^2) + It, \\ \lambda(Q^2) &= J + Kt. \end{aligned} \quad (\text{A.2})$$

	$D_0$ -type	$D_-$ -type
$A$	$4.818 \cdot 10^{-3}$	$8.07 \cdot 10^{-4}$
$B$	$-2.460 \cdot 10^{-3}$	$4.1 \cdot 10^{-5}$
$C$	$7.386 \cdot 10^{-4}$	$1.579 \cdot 10^{-4}$
$D$	$3.32 \cdot 10^{-6}$	$4.370 \cdot 10^{-5}$
$E$	$-2.23 \cdot 10^{-1}$	$-1.89 \cdot 10^{-1}$
$F$	$1.15 \cdot 10^{-2}$	$1.86 \cdot 10^{-2}$
$G$	$-5.3 \cdot 10^{-3}$	$-1.46 \cdot 10^{-2}$
$H$	$-6.66 \cdot 10^{-4}$	$-8.72 \cdot 10^{-4}$
$I$	$6.54 \cdot 10^{-3}$	$1.026 \cdot 10^{-2}$
$J$	$-5.113 \cdot 10^{-1}$	$-5.700 \cdot 10^{-1}$
$K$	$-7.10 \cdot 10^{-3}$	$-2.89 \cdot 10^{-3}$
$\Lambda_{\text{QCD}}$	173.2 MeV	230.4 MeV

Table 2: Coefficients defined in (A.2) of the parametrization (A.1)

The corresponding coefficients are given in Table 2. It is interesting to note that a small growth of  $\lambda$  with  $Q^2$  has to be taken into account.

It has to be stressed, that this parametrization is *only* valid within the range  $10^{-5} \leq x \leq 10^{-2}$  and  $0.8 \text{ GeV}^2 \leq Q^2 \leq 120 \text{ GeV}^2$ . On the one hand BFKL is not expected to be applicable even at the edges of this region. On the other hand we note, that the form of the ansatz has been tailored for this region only. The term  $\beta x$ , for example, will lead to wrong results for  $x > 10^{-2}$ .

## References

- [1] G. Altarelli and G. Parisi, Nucl. Phys. **B126**, 298 (1977).
- [2] V. N. Gribov and L. N. Lipatov, Yad. Fiz. **15**, 781 and 1218 (1972) [Sov. J. Nucl. Phys. **15**, 438 and 675 (1972)]; Yu. L. Dokshitzer, Zh. Eksp. Teor. Fiz. **73**, 1216 (1977) [Sov. Phys. JETP **46**, 641 (1977)].
- [3] M. Glück, E. Reya and A. Vogt, Z. Phys. **C53**, 127 (1992) and Phys. Lett. **B306**, 391 (1993).
- [4] M. Glück, E. Reya and M. Stratmann, Nucl. Phys. **B422**, 37 (1994).
- [5] M. Glück, E. Reya and A. Vogt, Z. Phys. **C67**, 433 (1995).
- [6] E. A. Kuraev, L. N. Lipatov and V. Fadin, Zh. Eksp. Teor. Fiz. **72**, 373 (1977) [Sov. Phys. JETP **45**, 199 (1977)]; Ya. Ya. Balitskij and L. N. Lipatov, Yad. Fiz. **28**, 1597 (1978) [Sov. J. Nucl. Phys. **28**, 822 (1978)].
- [7] C. Corianò and A. R. White, Phys. Rev. Lett. **74**, 4980 (1995).
- [8] M. Ciafaloni, Nucl. Phys. **B296**, 49 (1988); S. Catani, F. Fiorani and G. Marchesini, Nucl. Phys. **B336**, 18 (1990); R. Peschanski and S. Wallon, Phys. Lett. **B349**, 357 (1995).
- [9] J. C. Collins and R. K. Ellis, Nucl. Phys. **B360**, 3 (1991);
- [10] J. Kwieciński, A. D. Martin and P. J. Sutton, Univ. of Durham report DTP/95/22.
- [11] A. J. Askew, J. Kwieciński, A. D. Martin and P. J. Sutton, Mod. Phys. Lett. **A8**, No. 40, 3813 (1993).
- [12] A. J. Askew, J. Kwieciński, A. D. Martin and P. J. Sutton, Phys. Rev. **D49**, 4402 (1994).
- [13] E665 Coll., A. V. Kotwal, Fermi National Accelerator Laboratory report Fermilab-Conf-95/046-E, presented at the XXXth Rencontres de Moriond, March 1995.

- [14] H1 Coll., T. Ahmed *et al.*, Nucl. Phys. **B439**, 471 (1995); ZEUS Coll., M. Derrick *et al.*, Z. Phys. **C65**, 379 (1995).
- [15] H1 Coll., J. Dainton and G. Rädcl, talk given at the Workshop on Deep Inelastic Scattering and QCD, Paris, April 1995; ZEUS Coll., B. Foster and M. Lancaster, *ibid.*
- [16] M. Glück, E. Reya and A. Vogt, Z. Phys. **C48**, 471 (1990).
- [17] A. D. Martin, W. J. Stirling and R. G. Roberts, Rutherford Appleton Lab report RAL-95-021.
- [18] A. J. Askew, J. Kwieciński, A. D. Martin and P. J. Sutton, Phys. Rev. **D47**, 3775 (1993).
- [19] J. Kwieciński, Z. Phys. **C29**, 561 (1985).
- [20] A. Donnachie and P. V. Landshoff, Phys. Lett. **B296**, 227 (1992).
- [21] S. Catani, M. Ciafaloni and F. Hautmann, Nucl. Phys. **B366**, 657 (1991); S. Catani and F. Hautmann, Nucl. Phys. **B427**, 475 (1994).
- [22] D. Strozik-Kotlorz, Z. Phys. **C53**, 493 (1992).
- [23] H1 Coll., S. Aid *et al.*, DESY 95-081.
- [24] A. D. Martin, W. J. Stirling and R. G. Roberts, Phys. Rev. **D47**, 867 (1993).
- [25] P. J. Sutton, private communication.
- [26] B. Badelek and J. Kwieciński, Phys. Lett. **B295**, 263 (1992).
- [27] A. D. Martin, W. J. Stirling and R. G. Roberts, Phys. Rev. **D51**, 4756 (1995).

## Figure Captions

**Fig. 1** Gluon ladder with the quark box for deep-inelastic  $ep$  scattering attached. The momenta are shown on the left side of the Feynman diagram and the parts of the  $k_T$ -factorization theorem, Eq. (3), on the right.

**Fig. 2** AP inputs as indicated and the corresponding boundary conditions constructed via Eq. (6). The unmodified AP gluons are shown down to  $k_c^2 = 1 \text{ GeV}^2$ , whereas the IR treated inputs are continued below  $k_c^2$ .

**Fig. 3** Variations of the parameters. All curves are calculated at  $Q^2 = 15 \text{ GeV}^2$  with the  $D_0$ -type gluon input. The background  $C_{IP} x^{-0.08}$  has already been added to the BFKL curves and statistical and systematic errors of the data have been added in quadrature in this and all following figures. The legend for  $k_b^2$  is the same also for  $k_a^2$  and  $k_c^2$ .

**Fig. 4** Comparison of BFKL results, using MRSA-Low  $Q^2$  and GRV '92 LO gluon inputs, compared with data at several  $Q^2$ . The corresponding curves for the  $D_0$ -type gluon input is shown for comparison.

**Fig. 5** Low  $Q^2$  data of the Fermilab E665 experiment [13] and preliminary data of the HERA experiments [15] in comparison with our BFKL results. The background included in the  $D_0$ -type curves is separately displayed. Note that GRV '94 refers to the conventional dynamical results based on NLO AP evolutions of valence-like input parton densities [5].

**Fig. 6** As in Fig. 5 but using the HERA data of ref. [14].

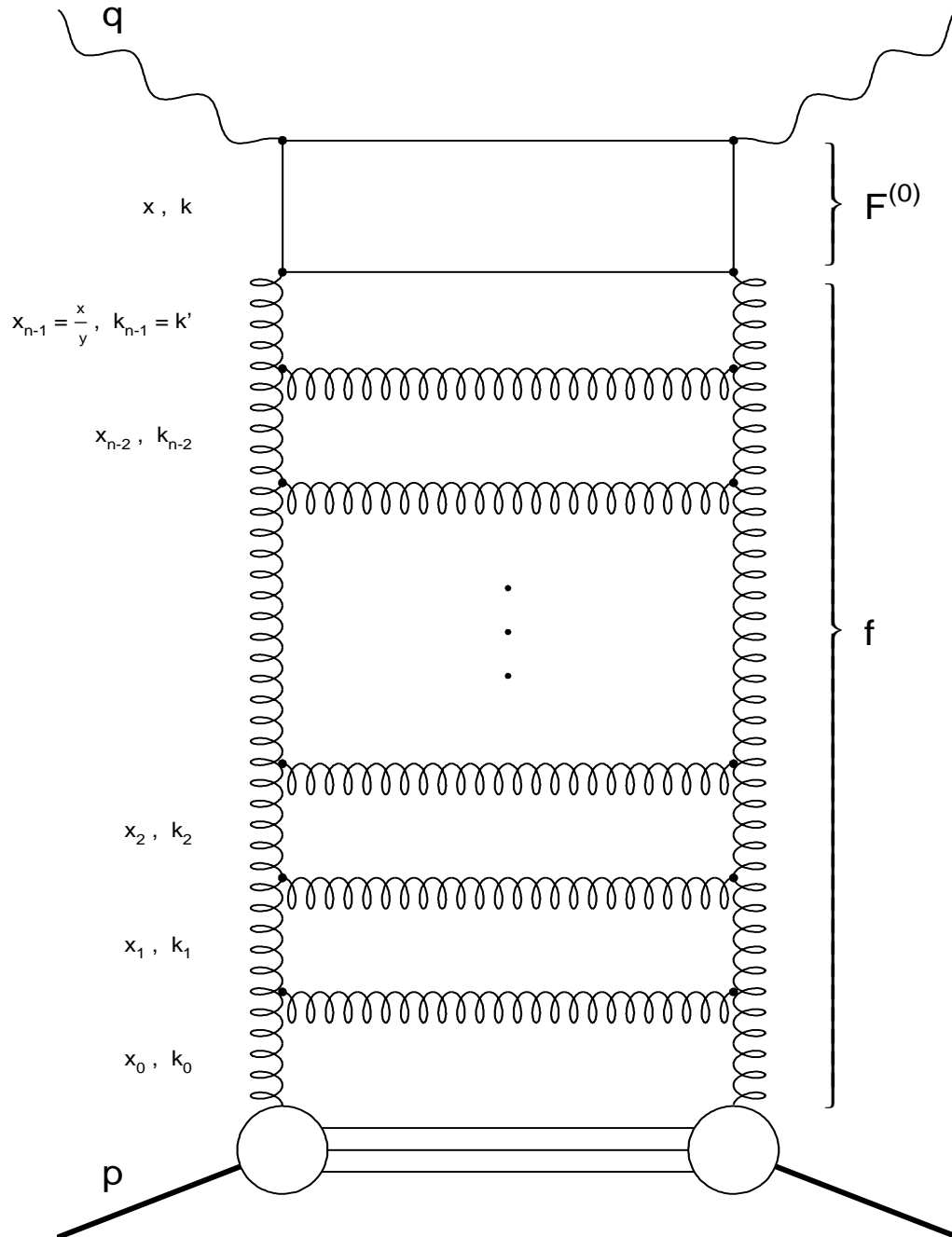


Fig. 1

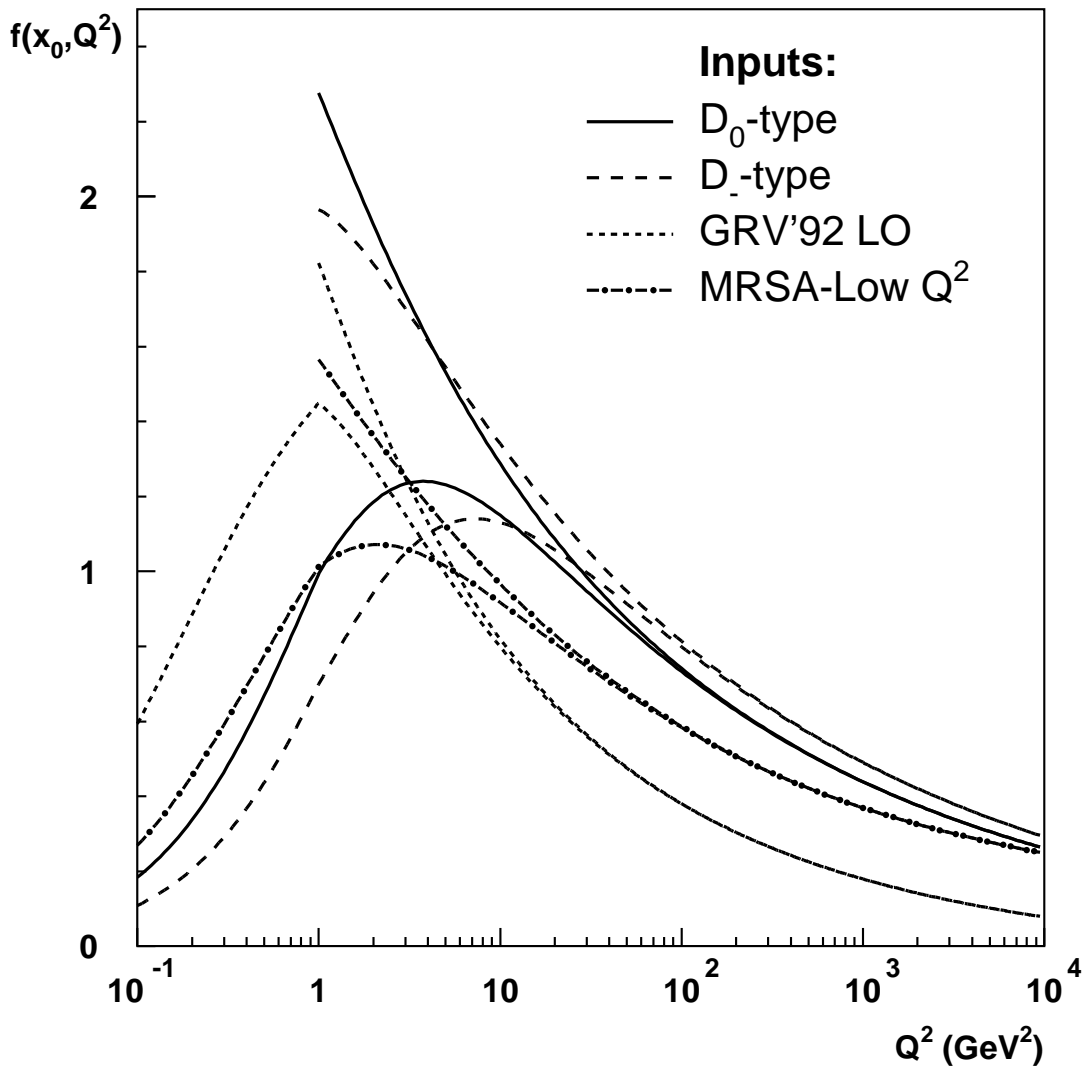


Fig. 2

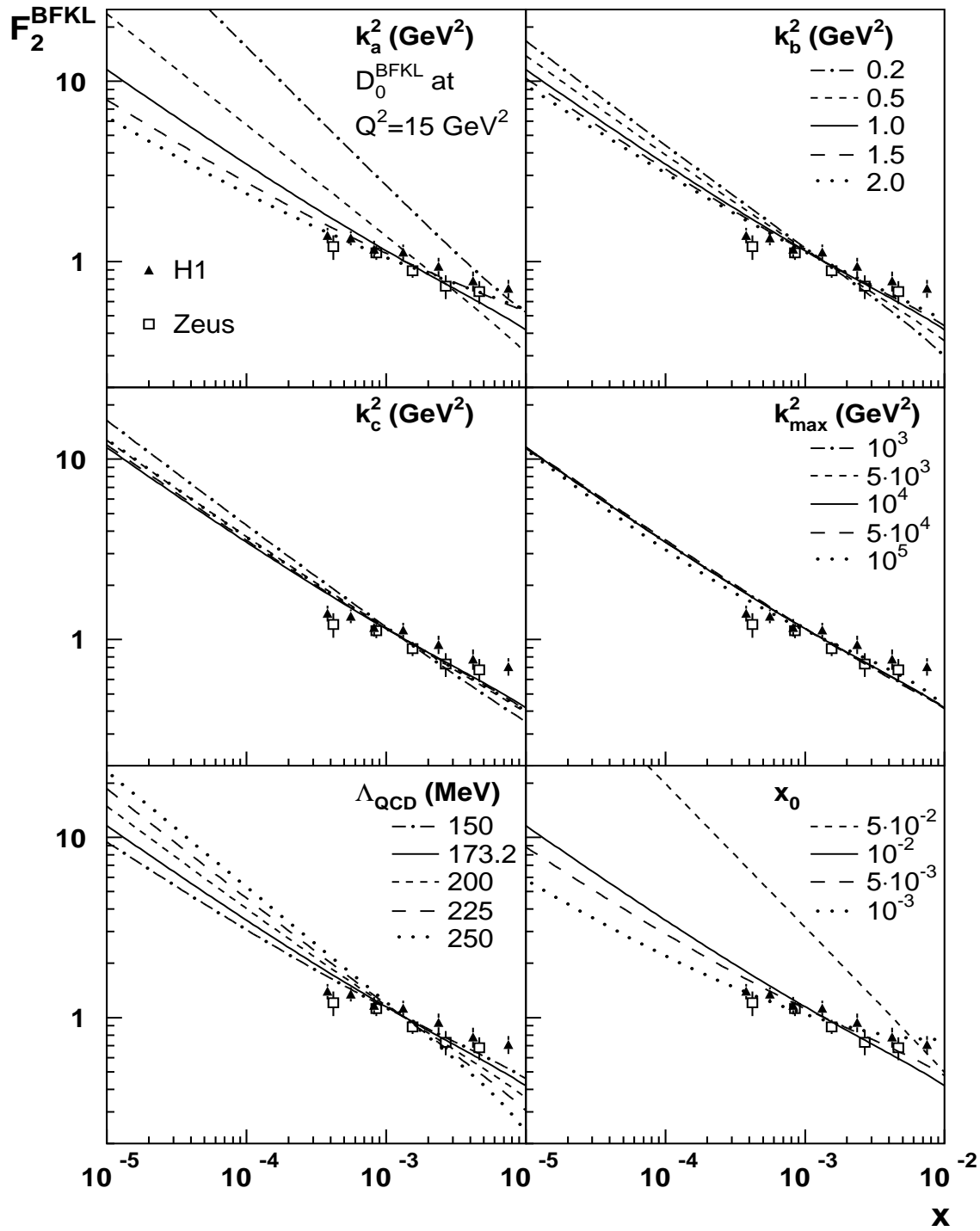


Fig. 3



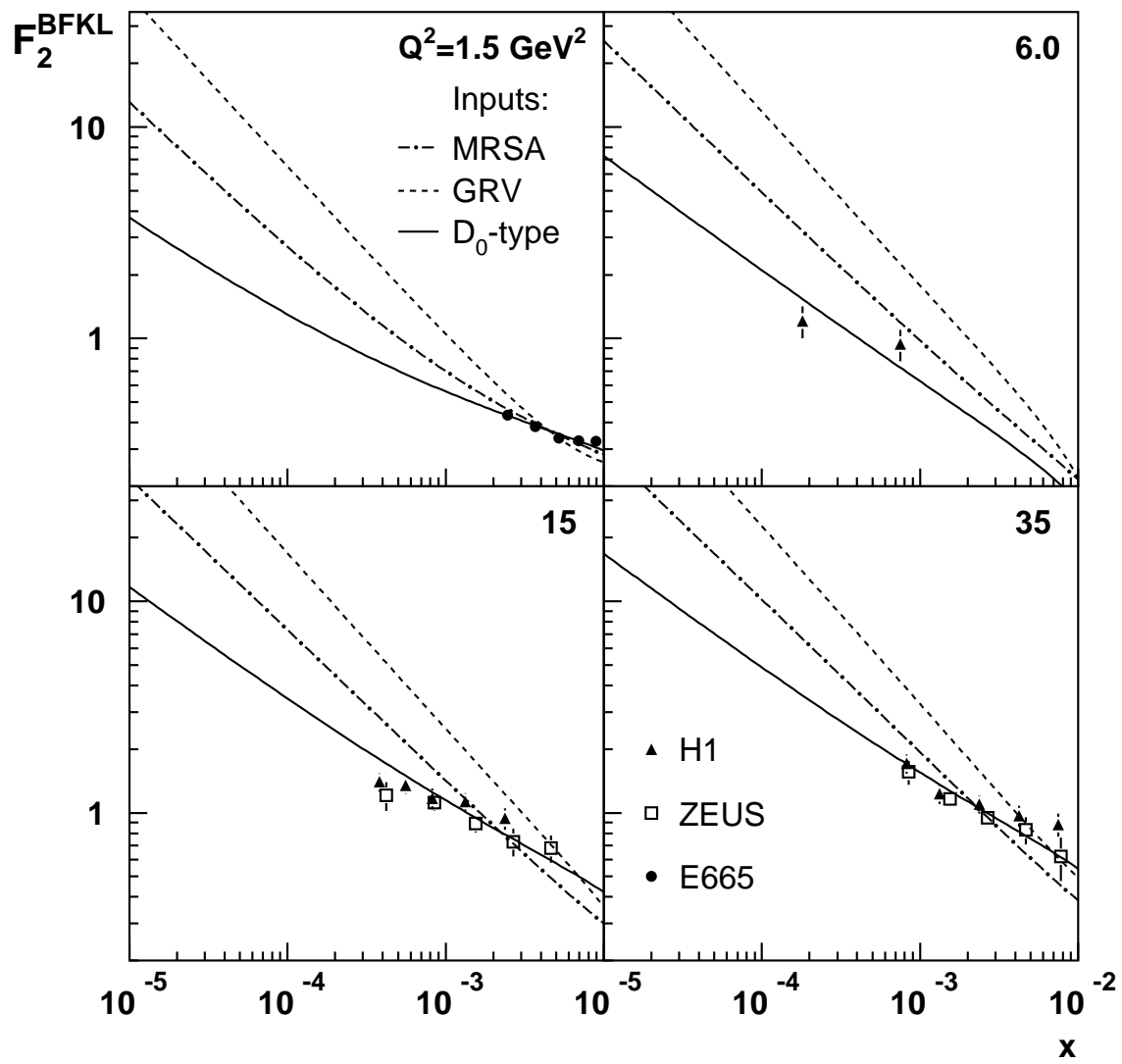


Fig. 4

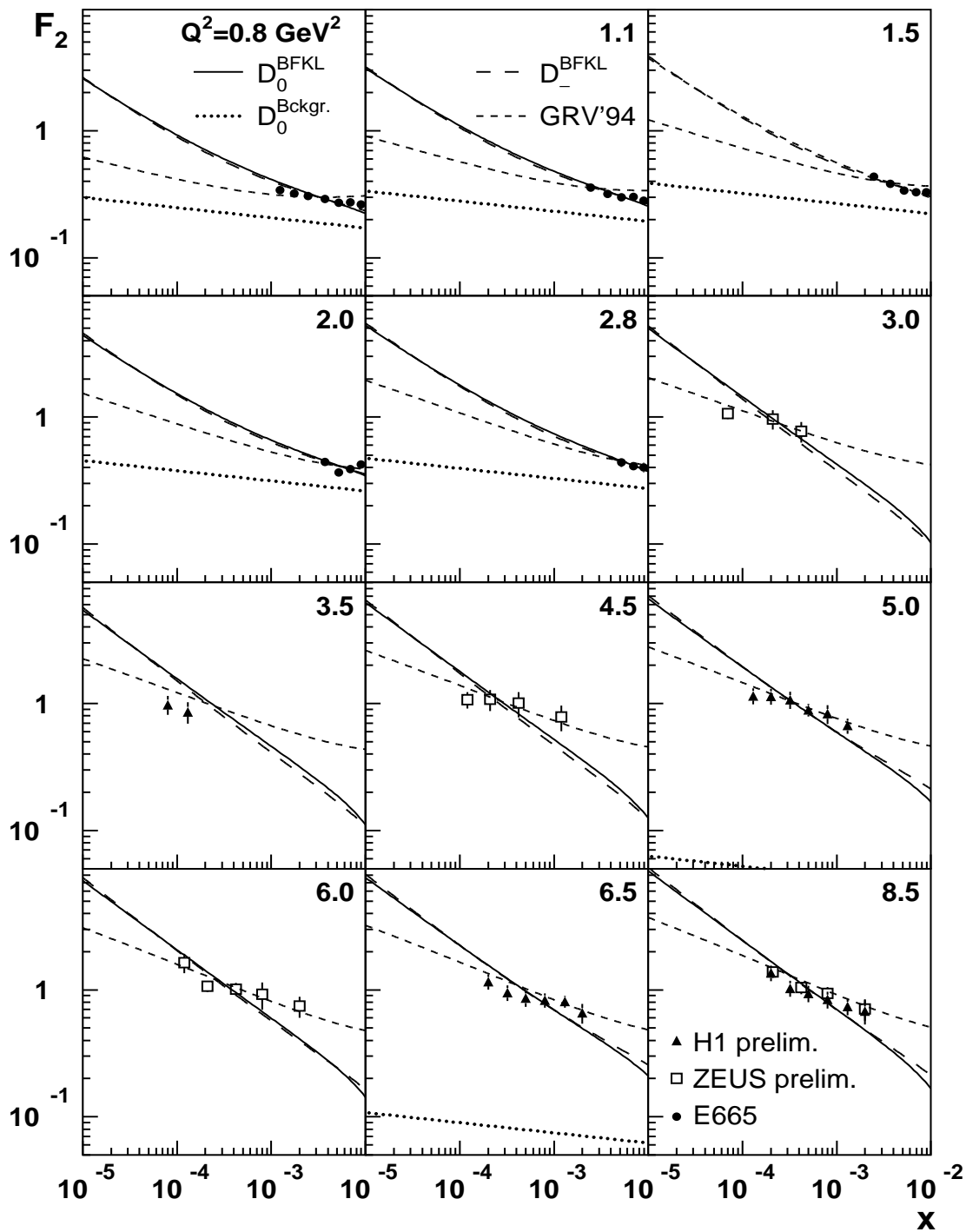


Fig. 5

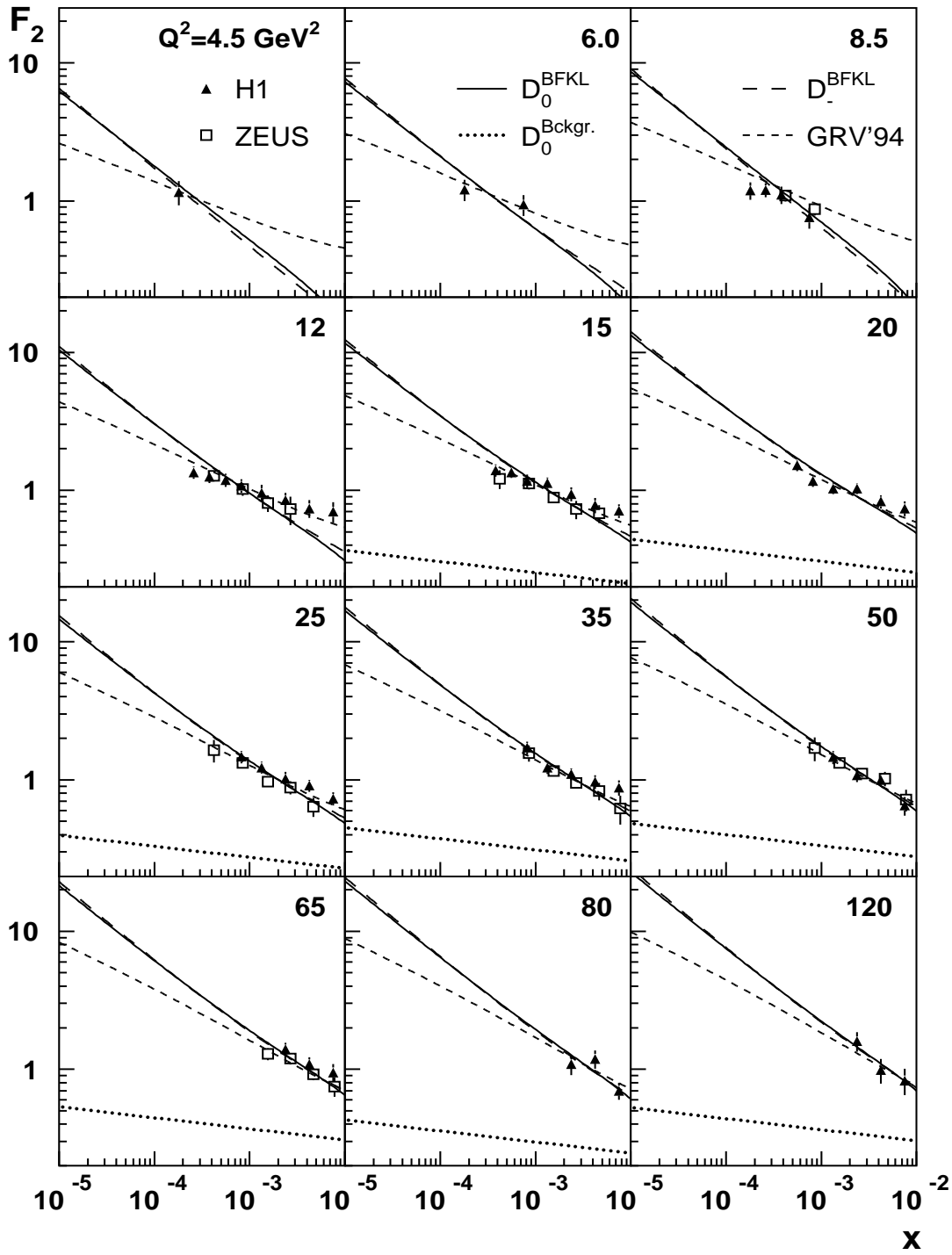


Fig. 6